Received: 24/05/2024 Revised: 01/08/2024 Accepted: 03/10/2024 Published: 04/12/2024

ORIGINAL ARTICLE

DOI 10.58430/jib.v130i4.60

INSTITUTE OF BREWING & DISTILLING

Impact of starch breakdown during germination and stewing on aroma formation in crystal malts

- Andrew R Foulkes[1]
- Irina Bolat[2]
- Chris Dodds[3]
- David J Cook[1]

[1] International Centre for Brewing Science, School of Biosciences, University of Nottingham, Sutton Bonington, Leicestershire LE12 5RD, UK.

[2] Boortmalt NV, Zandvoort 2, Haven 350/bus 1, 2030 Antwerp, Belgium.

[3] Department of Chemical and Environmental Engineering, University of Nottingham, University Park, Nottingham NG7 2RD, UK.

david.cook@nottingham.ac.uk

Abstract

Why was the work done: Crystal malts are used in brewing to add colour, flavour and mouthfeel to beers. In their manufacture, aroma compounds are formed through thermal flavour generation during roasting of stewed green malt. As part of a wider project to generate novel flavour extracts from roasted products, strategies to maximise aroma compounds in crystal malt were investigated.
How was the work done: Crystal malts were prepared at laboratory/micro-malting scale using a Box-Behnken experimental design where three parameters were varied: (i) germination time (4-6 days), (ii) stewing time at 65°C (1-24 hours) and (iii) roasting temperature (120-160°C). The major aroma compounds in the malts were quantified using Solid Phase Micro Extraction Gas Chromatography with Flame Ionisation detection.
What are the main findings: Response surface models are reported which predict the concentration of the quantitatively dominant compounds: acetic acid, furfural, 2-furanmethanol, maltol, HMF, 2,3-dihydro-3,5-dihydroxy-6-methyl-4(H)-pyran-4-one (DDMP), 5-methylfurfural and phenylacetaldehyde as a function of green malt germination time (2-6 days), stewing time (1-24 h) and roasting temperature (120-160°C). By optimising these factors, the concentration of bulk aroma compounds (sugar degradation products) increased up to sixfold relative to 'standard' conditions (four days germination, 1 hour stew at 65°C and roasting at 140°C). Optimal conditions for the formation of each compound are discussed in mechanistic terms. An image analysis method using cross polarised light microscopy was developed to quantify the degree of crystallinity of starch granules during stewing. Data indicate that under conventional manufacturing conditions there is a pool of ungelatinised starch in crystal malt kernels which represents an untapped source of aroma compound precursors.
Why is the work important: The results show that varying the production conditions changed the amounts and relative proportions of the main aroma compounds and hence the flavour of crystal malt. This may help maltsters understand differences in the flavour of products from different production facilities. Application of cross polarised light microscopy with image analysis revealed that a proportion of starch remains ungelatinised following standard industry stewing conditions. This demonstrates the potential to generate novel crystal malts with more flavour.

Keywords

crystal malt, thermal flavour generation, malt roasting, starch breakdown, germination, stewing

Introduction

Crystal malts are used in the brewing industry to impart beer with characteristic colour, aroma and mouthfeel (Sammartino 2015). They are produced by the roasting of germinated unkilned green barley malt which has been stewed by heating to 60-70°C in a closed/humidified environment for around one hour. The stewing process allows for amylolytic and proteolytic enzymes to digest the endosperm, creating precursors for colour and flavour formation during subsequent roasting. Starch breakdown creates dextrins and sugars in the endosperm, whilst protein breakdown creates amino acids which can catalyse the degradation of sugars via Maillard reaction pathways. Sugars are precursors to aroma compounds (Cerny 2008) as well as colour compounds that are polymerised or adducted to dextrins.

A schematic overview of crystal malt production is shown in Figure 1. In the initial stage, raw barley is steeped in water to increase the moisture level of the grain to 40-45%. The rise in moisture triggers a cascade of hormones from the embryo, signalling the aleurone layer to create hydrolytic enzymes (Sebree 1997). These enzymes are released into the starchy endosperm. Germination allows for the conversion of storage macromolecules into useful feedstocks to support plant growth. Breakdown of the protein matrix and starch granules leads to an increase in free sugars and amino acids over the course of germination. Smaller compounds are transported to the embryo for respiration or anabolism.

The biological process of breaking down large macromolecules into smaller subunits provides maltsters with an opportunity. By controlling germination, the maltster can produce a green malt with a high enough enzyme content but with limited carbohydrate loss (Sebree 1997). Prior to roasting, green malt is stewed at about 65°C to increase the conversion of starch into sugars and dextrins. During this period, the roasting drum is sealed so that moisture cannot escape and the amylolytic enzymes present can act on starch. A temperature of 65°C allows for maximal amylase activity without any significant denaturation (Briggs 1998).

Figure 1.

Crystal malt production. Steeping: Raw barley is submerged under water until the grain moisture is 40-45% which triggers germination. **Germination:** Grains are maintained at 40-45% moisture to allow modification of the endosperm and production of hydrolytic enzymes. **Stewing:** Germinated green malt is heated to 65°C in a sealed malting drum such that enzymes hydrolyse starch in the endosperm. **Roasting:** The roasting drum is vented and the temperature increased to dry the stewed green malt. This develops the desired colour and aroma of crystal malt.

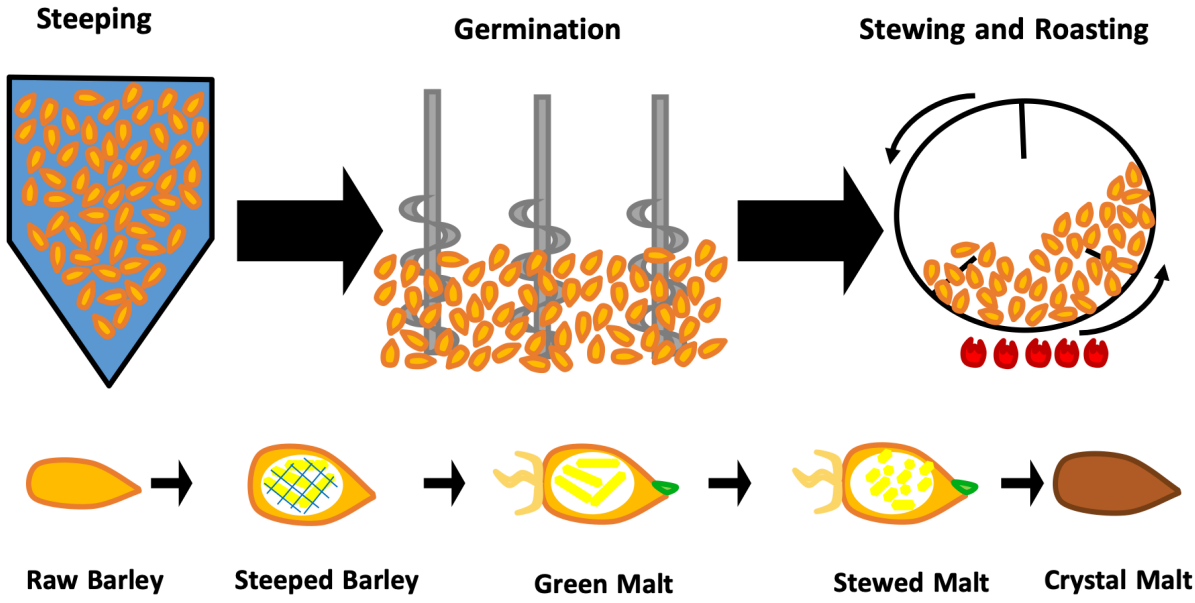

Stewing also gives enzymes greater access to starch due to gelatinisation. Barley starch consists of linear chains of amylose and branched chains of amylopectin (Zhu 2017). Starch granules in the barley endosperm contain amorphous and semi-crystalline layers, which display A-type diffraction patterns of light (Cornejo-Ramírez et al. 2018). Highly branched amylopectin is the main component of the amorphous layers (lamellae), which are inter-dispersed with more ordered crystalline regions where amylopectin side chains assemble into tightly packed helical structures. Some amylose chains are associated with these regions. By denying amylases access, this structure provides resistance to amylolysis of the starch granule by enzymatic attack (Karkalas et al. 1992). The crystallinity of an individual starch granule is affected by its size, amylose/amylopectin content, and association with lipids and other macromolecules (Cornejo-Ramírez et al. 2018). When heated to 65°C the structure becomes diffuse and water can enter and surround the individual chains, dissolving them and allowing access of amylolytic enzymes.

Following stewing, the grain is roasted. The temperature of the roasting drum is increased and moisture is allowed to escape. The temperature of the drum during the roasting phase is dependent on the required flavour and colour profile of the final product (Parr et al. 2021). Aroma compounds are generated thermally via the Maillard, caramelisation and pyrolytic pathways. The myriad of Maillard pathways to aroma formation are initiated by reactions between reducing sugars and amino acids. Amino acids are catalysts for an initial rearrangement before fragmentation and cyclisation creates oxygen containing heterocycles (Jousse et al. 2002). The Maillard pathways occur slowly at ambient temperatures but are much faster at high cooking and roasting temperatures. Caramelisation pathways allow for the thermal breakdown of sugars without the involvement of amino acids to facilitate the formation of intermediates. This pathway has a higher activation energy than Maillard pathways and requires temperatures above 120°C (Kroh 1994). Both the Maillard and caramelisation pathways produce similar oxygen containing heterocyclic compounds although in different quantities.

Further reactions of these aroma compounds lead to polymerisation or adduction to macromolecules that become colour active melanoidins (Bork et al. 2022).

Our previous work has shown the effect of roasting parameters - time, temperature and moisture - on the aroma of a range of roasted products used in brewing (Yahya et al. 2014; Parr et al. 2021). The aim of the research reported here was to maximise the concentration of aroma compounds in crystal malt products by manipulating the concentration of key precursors. The hypothesis was that 'standard' crystal malt processing is not optimised for aroma generation and, by manipulating the extent of germination of green malt, the length of stewing and the roasting temperature, more richly flavoured products could be developed. To better understand the breakdown of starch to aroma precursors during the stewing of green malt, a novel image analysis protocol was used to monitor the loss of starch crystallinity. This work enables, for the first time, aroma formation in crystal malts to be considered relative to the breakdown of starch during germination and stewing.

Materials and methods

Materials

Spring barley var. Laureate was supplied by Paul's Malt (Bury Saint Edmunds, UK) and winter var. Flagon was sourced from Crisp Malt (Fakenham, UK). High purity water from Water Purification Systems (SUEZ Water, Thame, UK) was used for all chemical analysis and for washing of glassware.

All chemical standards were >97.5% purity. 5-hydroxymethylfurfural (HMF), acetic acid, furfural, and 2-furanmethanol were supplied by Sigma Aldrich (Gillingham, UK). Maltol and sodium chloride were sourced from Fischer Scientific (Loughborough, UK).

Production of green malt

Green malt was produced in a Curio two-tank steep-germinator unit (Curio Malting, Milton Keynes, UK). Each tank consisted of four germination cages containing 300 g of raw barley (Laureate, Paul's Malt, UK). Raw barley was screened over a 2.25 mm slotted sieve to remove kernels that were undersized.

Steeping was performed at 17°C with three wet phases interrupted by two air rests (8 h wet, 16 h dry, 8 h wet, 16 h dry, 4 h wet). No steep aeration was used and the malting cages were turned automatically for one in every 10 minutes during steeping and germination. Germination was performed at 12°C for between 2-6 days (according to the experimental design). A low germination temperature was selected to favour the production of diastatic enzymes.

Stewing of green malt

Green malt was divided into 100 g portions in wide neck 500 mL Duran bottles. Green malt was kept at 5°C for a maximum of 6 hours before use. Bottles were placed in an oven at 65°C, with stewing time varyied between one and 24 hours.

Laboratory scale roasting

Crystal malt was roasted on a custom-built laboratory scale drum roaster (Parr et al. 2021). The roaster consists of a gas chromatograph oven (Hewlett Packard, 6890 series) and a barbeque rotisserie motor (GM012 model, BBQ Foukou, Koraskas, Cyprus) set through the oven wall. The spit controlled the rotation at 43 rpm of a roasting cage, attached by a push-fit connector. There was a solid baffle inside the cage to aid mixing. The roasting cage was placed in the oven and allowed to attemperate, at the roasting temperature (120-160°C), for 30 min before the addition of stewed malt. Stewed green malt (100 g) was added into the cage and connected to the rotating shaft. Malt was roasted for 40 min at the required temperature (120, 140 or 160°C).

On removal from the roaster, the crystal malt was transferred to an aluminium foil tray and submerged in liquid nitrogen. Frozen crystal malt was abraded over a 2 mm sieve to remove rootlets and allowed to return to room temperature. Samples were then sealed in foil bags and stored at -80°C until analysis.

Sample preparation for SPME-GC-FID

Crystal malt was ground using a Bühler-Miag disk mill (Uzwil, Switzerland) with the gap set to 0.2 mm (fine). Ground crystal malt (0.5 g ± 0.01 g) was added to an amber crimp top headspace vial (20 mL), and the weight taken. Sodium chloride solution (2 mL, 350 mg/mL) was then added. The internal standard 5-nonanone (50 µL, 800 mg/L) was added and the weight of the addition was taken so the internal standard concentration could be calculated. Vials were crimp sealed and stored at 5°C for at least 48 hours to equilibrate.

Aroma compound analysis using SPME-GC-FID

Samples were analysed using SPME-GC-FID using a Bruker Scion 456 Gas Chromatograph (Scion Instruments, Livingston, Scotland, UK) fitted with a ZB-Wax column (30 m x 0.25 mm ID 1.0 µm film thickness; Phenomenex, Macclesfield, UK). The GC was fitted with a flame ionisation detector. The vial seals were pierced by a DVB/CAR/PDMS SPME fibre (Merck, Darmstadt, Germany) and equilibrated for 45 min at 50°C. The fibre was desorbed using a split/splitless inlet - operated in splitless mode - at 220°C for 5 min. The oven temperature was held at 40°C for 10 mins and ramped at 4°C/min to 170°C. It was then ramped at 16°C/min to 230°C and held for 10 min.

Identification of aroma compounds

Linear retention indices of compound peaks were determined using liquid injection of an alkane series (C8-C40) from VWR International Ltd. The liquid injection conditions for the GC used the same column, oven temperature profile and detector. Retention indices were compared to database values for retention indices on a wax phase in the literature.

Five roasted crystal malt samples were further analysed using GC-MS to confirm peak assignment by mass spectra library matching in addition to linear retention index values of authentic standards. Volatiles were separated using a Trace 1300 gas chromatograph using the same column type and dimensions as for GC-FID together with the same inlet temperatures and oven heating regime. Effluent was analysed by EI-MS (Thermo Scientific, Waltham, MA, USA). EI-MS library matching was performed to verify peak identities.

Quantitation of aroma compounds

A stock solution of the stock solution was prepared containing 10 mg/mL of 5-hydroxymethylfurfural (HMF), acetic acid, furfural, 2-furanmethanol and maltol in water. Calibration headspace vials were prepared as described above but contained 0.5 g of milled pale malt, with 0, 10, 20, 30, 40, or 50 µL of the added external standard stock solution. Calibrant series were run before and after crystal malt samples. 2,3-dihydro-3,5-dihydroxy-6-methyl-4(H)-pyran-4-one (DDMP), 5-methylfurfural and phenylacetaldehyde were semi-quantified using the calibration curve for the standard with the closest retention time in each case.

Response Surface Modelling of aroma formation

A modified Box-Behnken design was used to determine the experimental conditions for germination time, stewing time, and roasting temperature (Table 1). The experimental design used the Design Expert 10 software (StatEase, Mn, USA). In all, 15 crystal malts were made. Germination time was 2, 4, or 6 days with stewing time of 1, 7, or 24 h; the centre point was modified from 12.5 due to constraints on working hours. This increased the error in model predictions at longer stewing times. However, the models had a precision of less than ± 2.5% across the design space, and the mean standard errors for maltol, HMF, furfural, and DDMP were 1.057, 1.105, 1.147, and 1.122 respectively. The roasting temperatures were 120, 140, and 160°C. The design space had three centre point repeats. Separate models were developed to predict the concentrations of each aroma compound across the design space.

ANOVA was used to determine the significance of the model terms. To avoid overfitting, non-statistically significant model terms ($p>0.05$) were removed, unless necessary for hierarchy.

Microscopic analysis of starch gelatinisation/loss of crystallinity

In addition to the response surface modelling, a better understanding of whether the design space incorporated the maximum potential for aroma compound formation was needed. That is, was there further scope to break down starch to yield precursors for flavour formation, or had a maximum yield been approached. Accordingly, novel microscopy/image analysis was developed to evaluate the extent of starch granule breakdown in green malt that was germinated and stewed to varying extents.

Production of ground stewed green malt

With the practical need for small samples, a 'nano malting regime' was used to malt 60 g of barley at a time for starch gelatinisation analysis. Raw barley (Flagon, Crisp Malt, UK) was steeped and germinated in square tubs at 15°C. Grain (60 g) was steeped with 120 mL of water in three wet phases with the following steep cycle: 8 h wet – 16 h dry – 8 h wet – 16 h dry – 4 h wet. After the final wet stand, the grain was drained and returned to Duran bottles (500 mL) and incubated at 15°C with mixing once a day to detangle rootlets. Germination time was either 4 or 6 days. Green malt was stewed in triplicate in 30 g portions in sealed vessels at 65°C for 0.25, 0.5, 0.75, 1, 2, 3, 5 and 8 hours. After stewing, the malt was ground using a Delonghi KG200 electric coffee grinder for 2 x 30 s, with stirring in between. Ground malt was stored at -80°C until analysis.

Preparation of samples for microscopy

Ground stewed green malt was suspended in water at 2% (w/w) and mixed on a Stuart SRT6D roller bed for one hour and used within three hours of preparation. Samples were vortexed before the suspended starch (10 µL) was placed on a microscope slide and covered with a coverslip with an attached polarising light filter.

Table 1.

Box-Behnken experimental design for crystal malt production.

Sample Number	Germination time (days)	Stewing Time (hours)	Roasting temperature (°C)
1	2	1	140
2	2	7	120
3	2	7	160
4	2	24	140
5	4	1	160
6	4	1	120
7	4	7	140
8	4	7	140
9	4	7	140
10	4	24	120
11	4	24	160
12	6	1	140
13	6	7	160
14	6	7	120
15	6	24	140

Microscopy

Microscopy was performed using a Nikon Eclipse Ci microscope with a 20 x lens. Images were captured using a Q imaging Retiga R1 camera and NIS elements software v5.11 (Laboratory Imaging s.r.o, Prague, Czech Republic). Images of starch were captured without the cross-polarised filter below the condenser. The same area was then captured using a polarising filter below the condenser at 90° to the coverslip filter. The lamp brightness was then increased until the total image intensity on the greyscale was $1.83 \times 10^8 \pm 0.05 \times 10^8$, where each pixel has a value between 0-255 and the total image pixels were 1409024. 15 pairs of images were captured per sample using at least three slides of suspended starch of each sample produced.

Image Analysis

Images were analysed using ImageJ2 (National Institute of Mental Health, Bethesda, Maryland, USA). The unpolarised image was used for automatic recognition of starch granules which were converted into binary to recognise edges of starch granules. The 'fill holes' function was used to fill in granules and those not completely identified were manually outlined. The 'watershed' function was used to separate overlapping starch granules. Particles analysed >50 pixels and outlines overlaid were sent to the Regions of Interest software manager. Outlines were overlaid onto the polarised image with intensity and area of starch coverage measured together with total intensity and image size. The image intensity for total image and individual starch granules was measured. For each image and starch granule the intensity ratio was calculated by dividing starch area by the mean background intensity of that image. The adjusted intensity values for each image (n=15) were averaged accounting for area covered by starch in each image.

Results and discussion

Impact of germination time, stewing time and roasting temperature on aroma formation

Acetic acid, furfural, 2-furanmethanol, maltol and 5-hydroxymethylfurfural were quantified using GC-SPME-FID. Further, DDMP, 5-methylfurfural, and phenylacetaldehyde were semi-quantified using the external standard calibration for the nearest eluting quantified compound. This method of quantification assumes that headspace samples have (prior to analysis) reached the equilibrium of the volatile analyte distribution between milled malt, saline solution, headspace and SPME fibre. It was also assumed that the milled pale malt was a representative matrix that would interact similarly with spiked standard concentrations of flavour volatiles as with the crystal malt products. Such assumptions resuklt in some error in absolute quantitation, but the method is appropriate for comparing the impact of process conditions on flavour formation. Further, the concentration of the analysed compounds are within the typical ranges reported in previous studies, particularly where similar process conditions were employed.

To determine how the processing of green malt prior to roasting affected the final concentrations of aroma compounds in crystal malt, a Box-Behnken experimental design was used. The design had three levels for each factor: germination time (2, 4, and 6 days), stewing time (1, 7 and 24 h) and roasting temperature (120, 140 and 160°C).

Details of the resulting models and their significant factors are reported in Table 1. The model coefficients reported are for the equation in 'coded terms' – i.e. for each variable the highest level across the design space is coded +1 and the lowest as -1. This gives a better comparison of the weighting of a factor numerically in the equation because the coefficients which are expressed are not distorted by the magnitude of the factor units. All the derived models were highly significant and with good predictive power (model R^2 = 0.89-0.99).

The coefficient for roasting temperature - a model term that included roasting temperature - had the highest magnitude in all models except for DDMP. As previously shown (Parr et al. 2021), this demonstrates that the concentration of aroma compounds in crystal malt are highly dependent on roasting temperature. This reflects the need for precursors of aroma compounds to overcome the activation energy to react. Higher roasting temperatures can lead to higher rates of formation but also higher rates of the loss of volatile aroma compounds. Therefore, the optimal roasting temperature to maximise the concentration of an aroma compound in finished crystal malt depends on the pathways for formation and loss (via onwards reactions, decomposition or volatility).

For all compounds, except 2-furanmethanol, there was an increase in concentration with the time of green malt germination (Table 2, factor A). Over the course of germination there is an increase in free amino acids, free sugars and diastatic power (Sebree 1997). This modification and generation of precursors for thermal flavour generation explains the increase in aroma compounds found after germinating for longer periods of time.

The released sugars and amino acids increase the pool of available precursors for aroma formation through caramelisation, Maillard chemistry or pyrolysis. A prolonged period of germination would also lead to a higher concentration of amylases (Vinje et al. 2015) which would impact on the initial rate of conversion of starch to sugars during the stewing part of crystal malt production.

With the exception of furfural, stewing time was a significant factor in all compound models (Table 2, factor B). Stewing time will also affect the concentration of aroma compound precursors before roasting. Stewing at 65°C allowed starch to be gelatinised and degraded. Gelatinisation exposes regions of the amylose and amylopectin chains, making them vulnerable to degradation by amylases resulting in dextrins and sugars such as maltose. Longer stewing times allow for greater conversion of starch into sugars that can then undergo thermally driven aroma forming reactions.

In most models, the magnitude of the model coefficients for germination and stewing time were of a similar order to the coefficient for roasting temperature. This indicated that germination and stewing time greatly impacted the final concentration of aroma compounds in crystal malt. Accordingly, extending the germination and stewing times beyond conventional manufacturing practice has the potential to generate crystal malt products with higher concentrations of aroma compounds, and particularly the bulk aroma compounds resulting from sugar degradation.

Response surface models for maltol, HMF, furfural and DDMP at each of the three different roasting temperatures are shown in Figures 2 and 3. There was a higher concentration of maltol in crystal malts that were roasted at higher temperatures with a plateauing or decrease when germination and stewing time were increased. However, this could be overridden by an increase in roasting temperature. The interaction between roasting temperature and the other two variables suggested that, at higher roasting temperatures, alternative pathways such as caramelisation may become more significant. These pathways would offer precursors that were increased by extended germination and stewing.

The concentrations of 5-hydroxymethylfurfural (HMF) in crystal malt showed a positive linear relationship with stewing time, germination time, and roasting temperature (Table 2, Figure 2). The model included a term for the interaction between germination time and stewing time. HMF is formed from the dehydration of hexose sugars, such as glucose and fructose through Maillard or caramelisation pathways (Kowalski et al. 2013). The higher concentration of HMF in crystal malt roasted at higher temperatures, showed that increasing the roasting temperature led to a larger increase in the rate of formation than rate of loss. Higher HMF concentrations in crystal malt, which had been germinated and stewed for a longer time, suggests that there is greater conversion of starch into maltose and maltotriose under these conditions. A lack of curvature in the response surface model, as compared with that for maltol, may mean that the formation of HMF at higher temperatures in the

Table 2.

Statistics for response surface models fitted to aroma compound concentration across the design space.
p-values are shown in brackets. Non-significant terms (p>0.05) are only included for model hierarchy. The models for furfural and 5-methylfurfural used a square root transformation prior to modelling.

	Response surface model coefficients and R^2									Model statistics	
Compound	A Germination time (2-6 days)	B Stewing time (1-24 h)	C Roasting temp. (120-160°C)	AB	AC	BC	A^2	B^2	C^2	Model type	Model R^2
Acetic acid	158 (0.0025)	152 (0.0031)	509 (<0.0001)	-	140 (0.0267)	-	-250 (0.0016)	-250 (0.0092)	-	Modified Quadratic	0.9705
Furfural	2.16 (<0.0001)	-	4.70 (<0.0001)	-	-	-	-	-	-	Modified Linear	0.9477
2-Furanmethanol	-	23.7 (<0.0001)	21.4 (0.0003)	-	-	-	-	-	-34.8 (0.0001)	Modified Quadratic	0.9030
Maltol	65.1 (0.0001)	66.8 (0.0001)	203 (<0.0001)	-	37.3 (0.0178)	39.3 (0.011)	-66.9 (0.0011)	-105 (0.0005)	-	Modified Quadratic	0.9900
HMF	405 (<0.0001)	285 (0.0001)	450 (<0.0001)	198 (0.0111)	-	183 (0.0162)	-	-	-	Modified 2 factor interaction	0.9563
DDMP	23.5 (<0.0001)	14.4 (0.0013)	-5.54 (0.1357)	-	-15.6 (0.0091)	-	-	-	-	Modified 2 factor interaction	0.8893
5-Methylfurfural	0.585 (0.0006)	0.254 (0.0423)	2.02 (<0.0001)	-	-	-	-0.580 (0.0068)	-	-0.545 (0.0095)	Modified Quadratic	0.9765
Phenylacetaldehyde	12.3 (0.0002)	6.43 (0.0065)	-8.07 (0.002)	-	-6.06 (0.038)	-	-9.11 (0.0078)	-11.6 (0.0106)	-16.5 (0.0003)	Modified Quadratic	0.9568

Figure 2.

Response Surface Models for maltol and HMF in crystal malt as a function of germination time (days), stewing time (hours) and roasting temperature. Dark and light red circles represent data points above and below the surface.

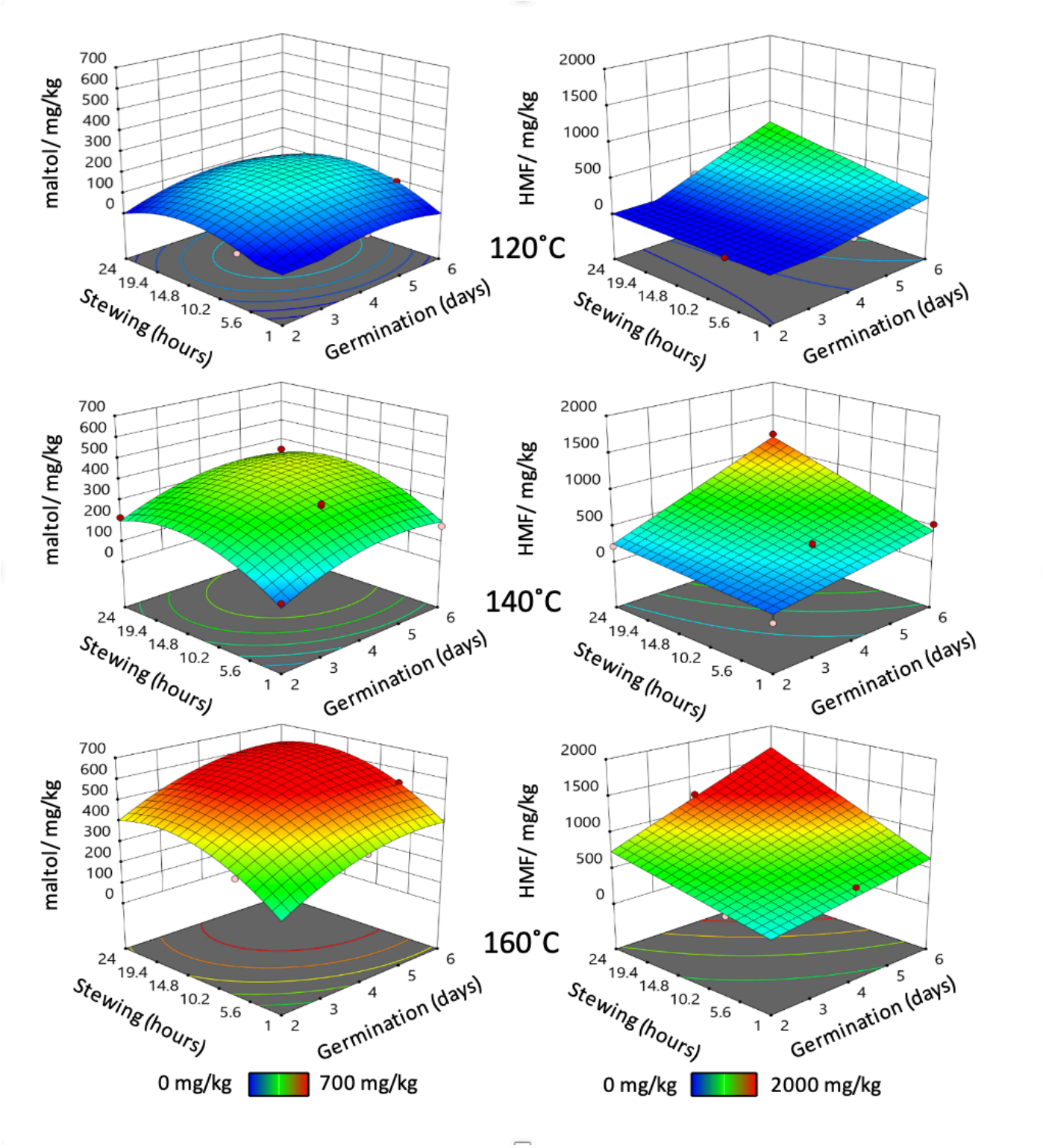

range (120-160°C) depended on caramelisation rather than the Maillard pathway, as the concentration was not limited by amino acid concentration as influenced by germination.

The response surface model for the concentration of furfural in crystal malt (Figure 3) used a square root transformation, indicating a greater variation in the results at higher concentrations (Hattab 2018). The model had a positive linear correlation with roasting temperature (0.872) and, less tightly, germination time (0.374). There was no statistically significant impact of stewing time. Furfural is formed from the dehydration of pentose sugars during caramelisation (Danon et al. 2014) and can also be formed from hexose sugars through Maillard and caramelisation reactions, as reported in the heating of sugar cane juice (Huang et al. 2023). The higher concentration of furfural in crystal malt roasted at higher temperatures indicates that the rate of formation increased faster than the rate of loss. Higher concentrations of furfural in crystal malt germinated for an extended period suggest the formation of more pentose sugar which are derived from the degradation of cell walls in the endosperm matrix (Sebree 1997). The lack of any statistically significant impact of stewing time suggests that the furfural concentrations in crystal malt were independent of starch breakdown into hexose sugars and were more likely to have been formed from pentoses.

For the formation of 2,3-dihydro-3,5-dihydroxy-6-methyl-4(H)-pyran-4-one (DDMP) (Figure 3), the model shows that the concentration was optimised at lower roasting temperatures. There was a positive, linear correlation between the concentration of DDMP in crystal malt and germination (0.726) and stewing times (0.467). Additionally, the term modelling the interaction between germination time and roasting temperature showed that germination time had a lower impact on DDMP concentration in crystal malt at higher roasting temperatures. DDMP is formed through Maillard and caramelisation pathways (Li et al. 2019; Li et al. 2020). DDMP, like HMF, is formed by 2,3-enolisation from the breakdown of hexose sugars. Indeed, the shared precursors to aroma compounds may suggest competition between pathways for the formation of these two compounds. A positive correlation between germination and stewing time is expected as both these factors increase the concentration of the hexose, maltose. A decrease in DDMP levels at higher roasting temperatures may be caused by the competing pathways that, at higher temperatures, result in the loss of DDMP through volatilisation or onward chemical reactions. In addition, roasting conditions result in the conversion of DDMP to DMHF (2,4-dihydroxy-2,5-dimethyl-3-(2H)-furanone) (Kim and Baltes 1996).

For the standard operating conditions - four days germination, 1 hour stewing and 140°C - the derived models were used to predict the maximum increase in concentration of each compound that could be obtained across the design space and the conditions under which this could be achieved (Table 3). By varying the processing conditions, the predicted maximum increase ranged from 1.6 fold (2-furanmethanol) to 6.1 fold (HMF). This suggests there is scope for increasing the concentration of aroma compounds in commercial crystal malts.

It is noteworthy that the changes in concentration were not uniform for the aroma compounds in crystal malt that were acievable (Table 3). The optimal conditions and increase in concentration for each compound are different. As previously suggested (Parr et al. 2021), changes in the processing conditions will lead to crystal malts with varied aroma profiles, which could be attractive for developing novel products with unique aroma. Sensory analysis would be required to determine how altered processing affects the perceived aroma of crystal malt, as opposed to measurement of the concentration of the compound.

Table 3 shows that, in general, five to six days of germination was optimal for the formation of aroma compounds due to the associated increase in aroma compound precursors. Over the course of germination there are many biochemical changes which could impact the final concentration of aroma compounds in crystal malt including: (i) the formation of hydrolytic enzymes; (ii) degradation of macromolecules into aroma compound precursors and (iii) structural changes to starch granules. It was only in the model for 2-furanmethanol that

Figure 3.

Response Surface Models for furfural and DDMP in crystal malt as a function of germination time (days), stewing time (hours) and roasting temperature. Dark and light red circles represent data points above and below the surface.

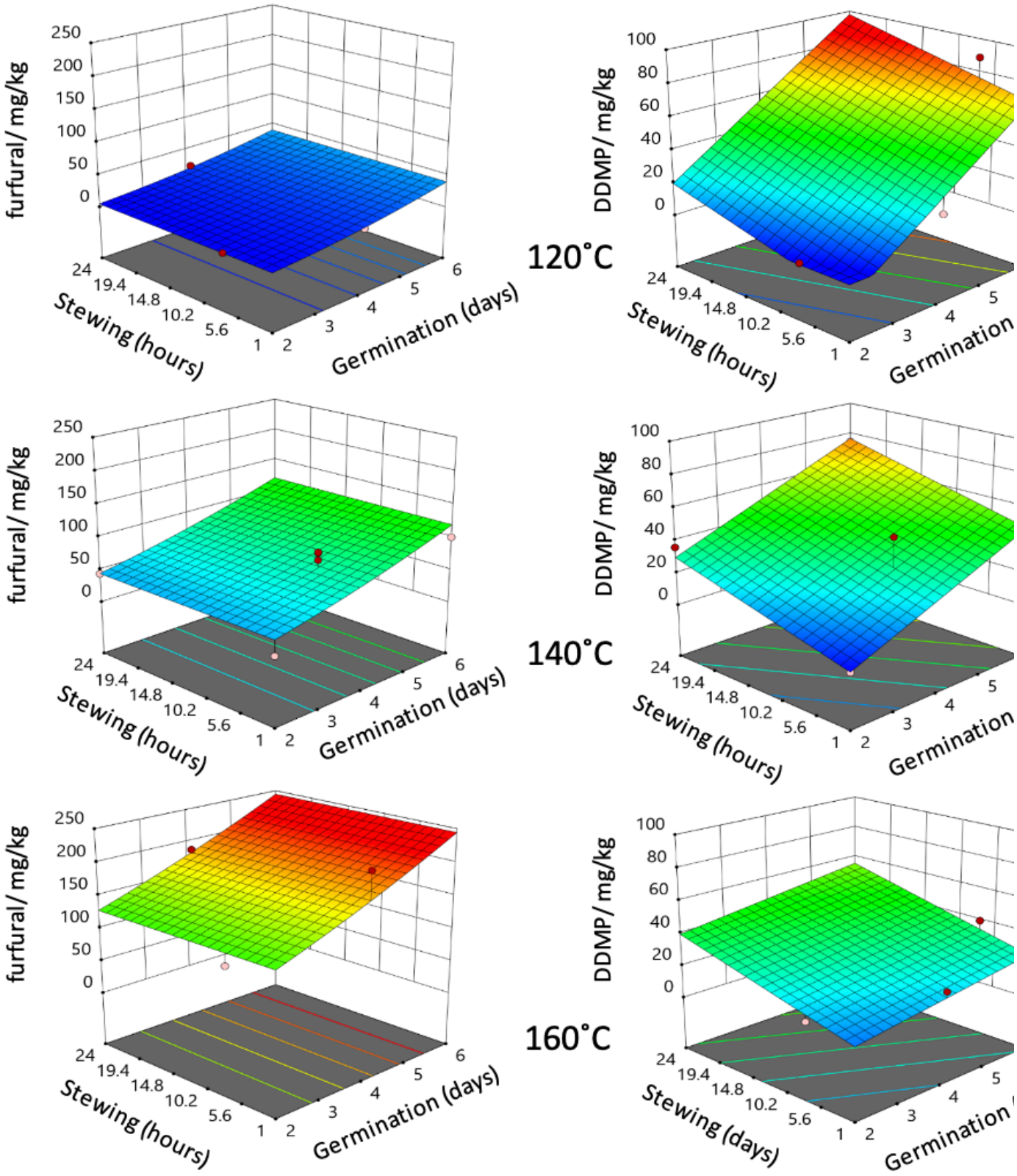

germination time was not a significant factor.

The optimal stewing time for individual compounds varied between 17-24 hours, suggesting that stewing as a variable has the potential to change the ratio of key flavour compounds in crystal malts, albeit that longer processing times in manufacturing would not always be commercially viable. Longer stewing time offers the potential to increase the concentration of aroma compounds (Table 3). This led to a consideration - as a function of stewing time - of the extent to which starch granules are broken down to generate sugars.

Starch gelatinisation during stewing using image analysis

In crystal malt processing, the majority of sugars are produced by amylolysis during the stewing phase (Briggs 1998). This is usually performed at around 65°C so that the amylases are not quickly denatured and can hydrolyse longer chain amylose and amylopectin into dextrins and maltose. This temperature is also required to ensure that starch is gelatinised, allowing the amylases to access amylose and amylopectin (Langenaeken et al. 2019). As sugar concentrations impact on the final level of aroma compounds in crystal malt, it follows that starch gelatinisation is important to their formation.

It is suggested that starch gelatinisation during the stewing of green malt has not been previously studied. Optimising gelatinisation before roasting could allow for greater conversion of starch into sugars, and result in an increase in the concentration of precursors to aroma compounds. Accordingly, a technique using cross-polarised light microscopy was devised to monitor the loss of crystallinity of starch granules during the stewing of green malt. This enabled the extent to which this conversion was complete to be assessed at different time points.

Green malt is maintained at a moisture content of 40-45% so as to allow germination to occur. In this environment the amount of free water that is available for the gelatinisation of starch is limited. It is therefore important to understand how the starch structure is taking up water during the stewing phase. To investigate this, green malt was germinated for four and six days and stewed for eight hours. The crystallinity of the starch granules was then determined using cross-polarised light microscopy (Ovalle et al. 2013).

Table 3.

Potential fold increase in the concentration of aroma compound through manipulation of germination time, stewing time and roasting temperature (predicted from models reported in Table 1).

Compound	Reference process predicted concentration (mg/kg)	Optimal germination time* (days)	Optimal stewing time* (hours)	Optimal roasting temperature* (˚C)	Highest predicted concentration (mg/kg)	Fold increase
Acetic acid	566	5.35	17.13	160	1585	2.80
Furfural	77	6.00	n/a	160	243	3.14
2-Furanmethanol	85	n/a	24.00	146	135	1.60
Maltol	199	5.53	18.29	160	640	3.21
HMF	277	6.00	24.00	160	1682	6.08
DDMP**	24	6.00	24.00	120	98	4.00
5-methylfurfural**	14	5.01	24.00	160	35	2.44
Phenylacetaldehyde**	38	5.61	24.00	132	64	1.66

Reference process: 4 days germination, 1 h stewing, 140°C.

* Optimal processing conditions were determined using the 'predicted maximum value' function for each model in Design Expert.
** Semi-quantified against the external standard peak with the closest retention time.

In this previous study with cross-polarised, light microscopy to detect gelatinisation, granules were categorised as either having a 'Maltese cross' or not (Ovalle et al. 2013). This suggests that gelatinisation is a binary process where granules are either gelatinised or not. However, water is taken into the granule gradually and the semi-crystalline structure is progressively disrupted. In this study, the scale of the 'degree of gelatinisation' was determined by comparing the light intensity of starch granules to the background intensity, to provide an 'intensity ratio' (see Table 4). Greater values of the intensity ratio are due to the higher birefringence in the more crystalline granules. Assigning each granule with a value enables the starch to be viewed as a population with frequency plots of the intensity ratios (Figure 4).

These plots showed a gradual shift of the population towards a gelatinised state as stewing progressed over eight hours – as can be seen by the distribution and the peak moving to lower intensity ratios reflecting the loss of crystallinity (Figure 4).

After germination and before stewing (time = 0), there was a large spread of intensity ratios for green malt germinated for either four and six days. This means that, although a median starch granule has an intensity ratio of approximately 1.10, there was a proportion of starch granules already accessible to degradation by amylases. As the green malt was stewed the frequency of the modal intensity ratio increased and shifted towards a smaller intensity ratio as the starch was gelatinised and became more homogeneous. After two hours, or shortly afterwards, most of the changes had occurred to the frequency curves.

Malt that had been germinated for six days displayed a faster shift towards lower intensity ratios with a larger skew in the same direction than was observed with malt germinated for four days (Figure 4). The greater shift suggests that more starch is available to amylolytic enzymes earlier on in the stewing phase when they are at their most active (Viader et al. 2021). Although a previous study of the physicochemical structure of barley starch during

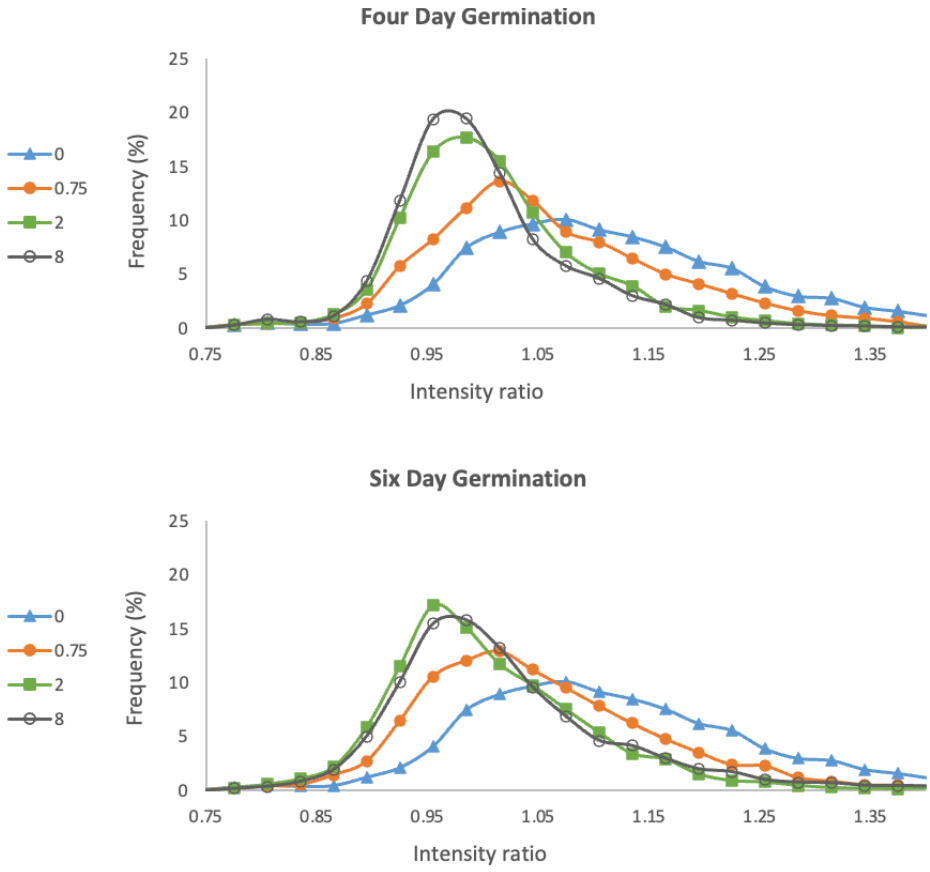

Figure 4.

Frequency distribution of the starch granule intensity ratio with varying durations of stewing (0-8 hours) at 65°C.

Table 4.

Microscopic images of starch granules with corresponding calculated intensity ratios.

A high ratio implies high retained crystallinity and birefringence.

Intensity ratio	Bright field	Cross polarised
1.722	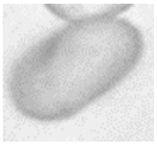	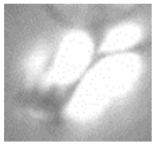
1.250	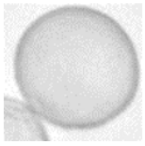	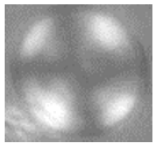
1.171	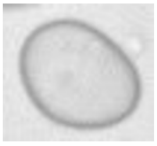	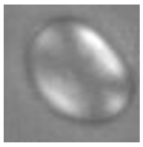
1.166	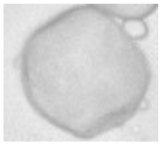	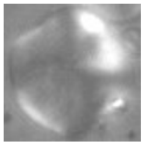
1.094		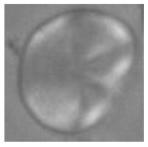
1.000	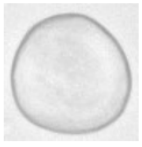	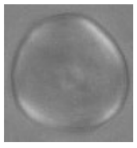
0.983		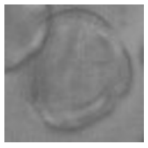
0.919		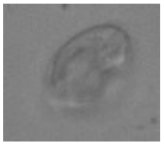

malting has shown an increased gelatinisation temperature at the start of germination, a decrease towards the end was also found (Contreras-Jiménez et al. 2019). Increased activity of the debranching enzyme, limit dextrinase may have impacted the rate of gelatinisation in green malt germinated for six days compared to four days, as limit dextrinase is rapidly converted to a free form between four to six days of germination (McCafferty et al. 2000). Although enzymic debranching of starch increases the crystallinity of starch upon cooling due to retrogradation (Pratiwi et al. 2018), attack from hydrolytic enzymes during stewing (before the starch has cooled), could have increased sugar formation and degraded debranched amylose chains available for retrogradation. After six days of germination, the capacity for degrading these amylose chains in the endosperm would have also been greater than after four days of germination due to higher concentrations of amylases (Vinje et al. 2015).

This faster rate of gelatinisation due to the longer stewing time may explain the increased concentration of aroma compounds after extended germination (Table 2). A faster rate of gelatinisation suggests that there is a higher concentration of substrate for amylases to act on before any denaturation can take place. A higher conversion of starch to sugars means there is a greater pool of aroma compound precursors before roasting. From this, a greater concentration of aroma compounds is formed during roasting and retained in the final product.

Starch gelatinisation could be a significant barrier to the formation of aroma compounds in crystal malt. Moisture levels in green malt at 40-45% suggest that the ratio of water to starch is limiting and could not completely gelatinise starch. This is not surprising as full gelatinisation of starch requires a stoichiometry of 14 molecules of water per hexose subunit (Donovan 1979). A 14:1 ratio would require a minimum moisture content of 48%, assuming 60% of the dry weight of green malt is starch and all the available water is utilised for gelatinisation, which is unrealistic. Therefore, a practical strategy to increase aroma compounds is to increase moisture levels in green malt prior to stewing, over and above normal industrial practice. However, this strategy

may be limited by the physical/biological constraints of the grain which have a finite volume for uptake of water and, if moisture is too high, germination stops. Indeed, a recent publication on the gelatinisation of starch in a brewery mash has shown there to be a limit on gelatinisation due to the increased solute concentration of hydrolysis products (De Schepper and Courtin 2022). Further, end-product inhibition of amylase will also limit hydrolysis during stewing (Lizotte et al. 1990). This inhibition mechanism protects the barley grain against degrading starch reserves faster than the embryo can take them up during germination. Increasing the moisture content of green malt during stewing would aid in overriding this mechanism and allow for greater conversion of starch to maltose.

Conclusions

The concentration of aroma compounds in crystal malt is not just dependent on roasting parameters (time and temperature) but also on the processing of the green malt before the high temperature phase of roasting. Extending the germination and stewing times of green malt allowed for a greater concentration of aroma compound precursors and a bigger compliment of hydrolytic enzymes to release them during stewing. This increase in aroma compound precursors was found to increase the concentration of aroma compounds sixfold under experimental conditions.

There is potential to increase the concentration of sugars in green malt prior to roasting through maximising starch gelatinisation. Current methods of processing crystal malt do not fully gelatinise starch, which was demonstrated here using a novel image analysis technique. This represents potentially an untapped source of aroma compounds in the form of ungelatinised starch which is inaccessible to amylolysis. Further increases in aroma compound concentrations in crystal malt may depend on overcoming this, possibly though increasing the moisture content of green malt.

Author contributions

Andrew Foulkes: Research and formal analysis. Writing (original draft).
Irina Bolat: Funding and supervision. Review of manuscript.
Chris Dodds: Funding acquisition and supervision. Review of manuscript.
David Cook: Funding acquisition, supervision and conceptualisation. Writing (review and editing).

Acknowledgements

This research was supported by the Engineering and Physical Sciences Research Council (EPSRC) and Boortmalt NV.

Conflict of interest

The authors declare there are no conflicts of interest.

References

Bork LV, Haase PT, Rohn S, Kanzler C. 2022. Formation of melanoidins – Aldol reactions of heterocyclic and short-chain Maillard intermediates. *Food Chem* 380:131852-131852. https://doi.org/10.1016/j.foodchem.2021.131852

Briggs DE. 1998. *Malts and Malting*. London: Blackie Academic & Professional.

Cerny C. 2008. The aroma side of the Maillard reaction. *Ann N Y Acad Sci* 1126:66-71. https://doi.org/10.1196/annals.1433.011

Contreras-Jiménez B, Del Real A, Millan-Malo BM, Gaytán-Martínez M, Morales-Sánchez E, Rodríguez-García ME. 2019. Physicochemical changes in barley starch during malting. *J Inst Brew* 125:10-17. https://doi.org/10.1002/jib.547

Cornejo-Ramírez YI, Martínez-Cruz O, Del Toro-Sánchez CL, Wong-Corral FJ, Borboa-Flores J, Cinco-Moroyoqui FJ. 2018. The structural characteristics of starches and their functional properties. *CyTA: J Food* 16:1003-1017. https://doi.org/10.1080/19476337.2018.1518343

Danon B, Marcotullio G, De Jong W. 2014. Mechanistic and kinetic aspects of pentose dehydration towards furfural in aqueous media employing homogeneous catalysis. *Green Chem* 16:39-54. https://doi.org/10.1039/c3gc41351a

De Schepper CF, Courtin CM. 2022. High mashing thickness negatively influences gelatinisation of small and large starch granules and starch conversion efficiency during barley malt brewing. *Food Hydrocoll* 131:107745. https://doi.org/10.1016/j.foodhyd.2022.107745

Donovan JW. 1979. Phase transitions of the starch-water system. *Biopolymers* 18:263-275. https://doi.org/10.1002/bip.1979.360180204

Hattab MW. 2018. On the use of data transformation in response surface methodology. *Qual Reliab Eng Int* 34:1185-1194. https://doi.org/10.1002/qre.2317

Huang H, Chen J, Zheng M, Zhang L, Ji H, Cao H, Dai F, Wang, L. 2023. Precursors and formation pathways of furfural in sugarcane juice during thermal treatment. *Food Chem* 402:134318-134318. https://doi.org/10.1016/j.foodchem.2022.134318

Jousse F, Jongen T, Agterof W, Russell S, Braat P. 2002. Simplified kinetic scheme of flavor formation by the Maillard reaction. *J Food Sci* 67:2534-2542. https://doi.org/10.1111/j.1365-2621.2002.tb08772.x

Karkalas J, Tester RF, Morrison WR. 1992. Properties of damaged starch granules. I. Comparison of a micromethod for the enzymic determination of damaged starch with the standard AACC and Farrand methods. *J Cereal Sci* 16:237-251. https://doi.org/10.1016/S0733-5210(09)80087-8

Kowalski S, Lukasiewicz M, Duda-Chodak A, Zięć G. 2013. 5-Hydroxymethyl-2-Furfural (HMF) – Heat-induced formation, occurrence in food and biotransformation – a review. *Pol J Food Nutr Sci* 63:207-225. https://doi.org/10.2478/v10222-012-0082-4

Kroh LW. 1994. Caramelisation in food and beverages. *Food Chem* 51:373-379. https://doi.org/https://doi.org/10.1016/0308-8146(94)90188-0

Langenaeken NA, De Schepper CF, De Schutter DP, Courtin CM. 2019. Different gelatinization characteristics of small and large barley starch granules impact their enzymatic hydrolysis and sugar production during mashing. *Food Chem* 295:138-146. https://doi.org/10.1016/j.foodchem.2019.05.045

Li H, Tang X-Y, Wu C-J, Yu S-J. 2019. Formation of 2,3-dihydro-3,5-Dihydroxy-6-Methyl-4(H)-Pyran-4-One (DDMP) in glucose-amino acids Maillard reaction by dry-heating in comparison to wet-heating. *Lebensm Wiss Technol* 105:156-163. https://doi.org/10.1016/j.lwt.2019.02.015

Li T-X, Ji L-B, Jiang Z-R, Geng Z-Z, Shentu H-Q, Liu M-C, Xie Y-F, Hu J, Liu Y-F, Li D-L. 2020. Caramel products of glucose with water during heating process and their bioactivities. *Int J Food Pro* 23:971-978. https://doi.org/10.1080/10942912.2020.1770788

Lizotte PA, Henson CA, Duke SH. 1990. Purification and characterization of pea epicotyl beta-amylase. *Plant Physiol Suppl* (Bethesda) 92:615-621. https://doi.org/10.1104/pp.92.3.615

McCafferty CA, Perch-Nielsen N, Bryce JH. 2000. Effects of aerobic and anaerobic germination on the debranching enzyme, limit dextrinase, in barley malt. *J Am Soc Brew Chem* 58:47-50. https://doi.org/10.1094/ASBCJ-58-0047

Ovalle N, Cortés P, Bouchon P. 2013. Understanding microstructural changes of starch during atmospheric and vacuum heating in water and oil through online in situ vacuum hot-stage microscopy. *Innov Food Sci Emerg Technol* 17:135-143. https://doi.org/10.1016/j.ifset.2012.11.006

Parr H, Bolat I, Cook D. 2021. Modelling flavour formation in roasted malt substrates under controlled conditions of time and temperature. *Food Chem* 337:127641. https://doi.org/10.1016/j.foodchem.2020.127641

Pratiwi M, Faridah DN, Lioe HN. 2018. Structural changes to starch after acid hydrolysis, debranching, autoclaving-cooling cycles, and heat moisture treatment (HMT): A review. *Starch* 70. https://doi.org/10.1002/star.201700028

Sammartino M. 2015. Specialty malt: A summary. *Tech Q Master Brew Assoc Amer* 52:191-194. https://doi.org/10.1094/TQ-52-4-0930-01

Sebree BR. 1997. Biochemistry of malting. T*ech Q Master Brew Assoc Amer* 34:148-151.

Viader RP, Yde MSH, Hartvig JW, Pagenstecher M, Carlsen JB, Christensen TB, Andersen ML. 2021. Optimization of beer brewing by monitoring α-amylase and β-amylase activities during mashing. *Beverages* 7:13. https://doi.org/10.3390/beverages7010013

Vinje MA, Duke SH, Henson CA. 2015. Comparison of factors involved in starch degradation in barley germination under laboratory and malting conditions. *J Am Soc Brew Chem* 73:195-205. https://doi.org/10.1094/ASBCJ-2015-0318-01

Yahya H, Linforth RS, Cook DJ. 2014. Flavour generation during commercial barley and malt roasting operations: a time course study. *Food Chem* 145:378-387. https://doi.org/10.1016/j.foodchem.2013.08.046

Zhu F. 2017. Barley starch: composition, structure, properties, and modifications. *Compr Rev Food Sci Food Saf* 16:558-579. https://doi.org/10.1111/1541-4337.12265